Biochimica et Biophysica Acta 1838 (2014) 2539–2546

Contents lists available at ScienceDirect

Biochimica et Biophysica Acta

journal homepage: www.elsevier.com/locate/bbamem

Substrate binding to the multidrug transporter MepA

Christian Banchs [1], Sandra Poulos [1], Waroot S. Nimjareansuk, Ye Eun Joo, Salem Faham *

Department of Molecular Physiology and Biological Physics, University of Virginia School of Medicine, Charlottesville, VA, 22903, United States

ARTICLE INFO

Article history:
Received 19 February 2014
Received in revised form 11 June 2014
Accepted 16 June 2014
Available online 23 June 2014

Keywords:
Efflux
Drug resistance
Detergent effect
Membrane proteins
Drug design

ABSTRACT

MepA is a multidrug transporter from *Staphylococcus aureus* that confers multidrug resistance through the efflux of a wide array of hydrophobic substrates. To evaluate the ability of MepA to recognize different substrates, the dissociation constants for interactions between MepA and three of its substrates (acriflavine (Acr), rhodamine 6G (R6G), and ethidium (Et)) were measured. Given that MepA is purified in the presence of detergents and that its substrates are hydrophobic, we examined the effect of the detergent concentration on the dissociation constant. We demonstrate that all three substrates interact directly with the detergent micelles. Additionally, we find the detergent effect on the K_D value to be highly substrate-dependent. The K_D value for R6G is greatly influenced by the detergent, whereas the K_D values for Acr and Et are only modestly affected. The effect of the inactive D183A mutant on binding was also evaluated. The D183A mutant shows lower affinity toward Acr and Et.

1. Introduction

Multidrug resistance (MDR) poses a growing health concern with the rise of pathogenic bacteria that are resistant to antibiotics. The efflux of drugs by transporters is a common mechanism for the emergence of drug resistance [1,2]. Five superfamilies of multidrug exporters have been identified so far: the small multidrug resistance (SMR) family [3], the resistance nodulation and cell division family (RND) [4], the ATP binding cassette family (ABC) [5], the major facilitator family (MFS) [6], and the multidrug and toxic compound extrusion (MATE) family [7]. The MATE family was the last to be identified and is the least well characterized. NorM from *Vibrio parahaemolyticus* was the first member of the MATE family to be identified for its ability to confer a MDR phenotype [8]. In microorganisms, several MATE proteins have been found to confer MDR through efflux of a wide variety of compounds [9–17]. A number of MATE structures have been determined recently [18–20] with some in complex with their substrates.

MepA is a member of the MATE family that was found to be overexpressed in *Staphylococcus aureus* (*S. aureus*) strains with increased resistance to various antibiotic compounds [21]. It was shown that over expression of MepA confers MDR in *S. aureus* [22]. Similar to other MATE transporters, MepA exports a variety of compounds that are structurally diverse yet share common characteristics. Typically the MepA substrates are hydrophobic, aromatic, and carry a delocalized positive charge. These substrates include: acriflavine (Acr), ethidium (Et), rhodamine 6G (R6G), benzyl alkonium, crystal violet, tetraphenylphosphonium (TPP), 4-6-diamidino-2-phenylindole (DAPI), dequalinium, and pentamidine [22]. Currently, there are no biochemical characterizations of MepA or any information on binding to substrates.

In order to shed light on the ability of MepA to recognize and export a wide array of substrates here we measured the binding of MepA to three of its substrates: namely, acriflavine (Acr), ethidium (Et), and rhodamine 6G (R6G). Due to the inherent hydrophobic nature of these substrates and the fact that MepA is purified in the presence of detergent, we also carried out a detailed study on the influence of the detergent concentration on binding of these three substrates to MepA. Direct interactions between the DDM micelles and the three substrates were evaluated. We also measured the effect of the inactive D183A mutant on substrate binding [23]. This mutation is expected to be far from the substrate binding site, based on a MepA model that is derived from a homologous MATE structure [23]. All three substrates are intrinsically fluorescent, which allowed the use of fluorescence polarization (FP) to monitor their binding to the protein. In the case of Et, fluorescence enhancement was an additional tool used to monitor binding to MepA. The detergent selected for this study was dodecyl-maltoside (DDM), since it is a commonly used detergent, and because many membrane proteins are stable in DDM [24,25].

2. Materials and methods

2.1. MepA cloning, expression and purification

Wild-type MepA was cloned from the Mu 50 strain of *S. aureus* into a pBAD expression vector with an N-terminal 12-His tag. Protein expression was carried out in *E. coli* Top10 cells as recommended (tools.lifetechnologies.com/content/sfs/manuals/pbad_man.pdf) by Invitrogen [26].

* Corresponding author.
E-mail address: sf3bb@virginia.edu (S. Faham).
[1] These authors contributed equally to this work.

http://dx.doi.org/10.1016/j.bbamem.2014.06.013
0005-2736/

For purification, the cells were resuspended in (20 mM Tris pH 8.0, 150 mM NaCl, and 5% (v/v) glycerol) (buffer A). The cells were ruptured by three passes through an M110-P microfluidizer (Microfluidics) at 20 k psi, and the membranes were isolated by ultra-centrifugation for 1 h at 42 k rpm (204,526 g) in an Optima LE-80 k ultracentrifuge (Beckman Coulter) using a Ti-45 rotor, after removing cell debris with a low speed centrifugation. Frozen membranes were solubilized in buffer A containing 2% (w/v) DDM detergent (Affymetrix) and 2 mM β-mercaptoethanol (BME). The concentration of DDM is reported throughout the manuscript in terms of a (w/v) percentage. The DDM-solublized membranes were again centrifuged at 42 k rpm (204,526 g) in an Optima LE-80 k ultracentrifuge (Beckman Coulter) using a Ti-45 rotor for 1 h at 4 °C. 10 mM imidazole and 2 ml of Ni-NTA resin were added to the supernatant and the combined mixture was kept stirred at 4 °C for 1 h. The resin was then applied to a gravity flow column and washed with 30 ml of (50 mM Tris pH 8.0, 150 mM NaCl, 0.02% DDM, 2 mM BME) (buffer B) with 30 mM imidazole, followed by another 30 ml wash step using the same buffer B but with 50 mM imidazole. Protein was eluted from the column in buffer B plus 450 mM imidazole (Fig. S1). The eluted protein was concentrated by centrifugation using 50 k MWCO Amicon Ultracel® (Milipore). The protein sample was then applied to a Superdex 200 10/300 GL size exclusion column (SEC; GE Healthcare) equilibrated with buffer B using an AKTA Purifier chromatography system (GE Healthcare). The peak fractions were collected and analyzed with SDS-PAGE to confirm sample purity (Fig. S1). The fractions were then combined, concentrated, flash frozen under liquid nitrogen and stored at −80 °C. For binding assays, the protein was thawed and ultracentrifuged for 1 h at 60 K (127,814 g) in a Beckman optima ultracentrifuge using a TLA120.1 rotor, to remove any aggregates. The protein concentration was determined again, after ultracentrifugation. Purification of MepA in C12E8 was carried out in the same manner as described for DDM, except that Anapoe-C12E8 was used in place of DDM.

2.2. DDM concentration determination

The concentrations of DDM in concentrated protein samples were measured as described by Urbani [27]. Briefly, 1.0% (w/v) phenol solution in concentrated sulfuric acid was prepared and kept on ice. DDM standards were prepared with concentrations ranging from 0 to 2.0%. DDM standards and the protein samples were dispensed in triplicate aliquots of 10 μl into disposable borosilicate tubes (Fisherbrand), and 1 ml of the phenol/sulfuric acid mixture was added to each and vortexed. The tubes were then covered with parafilm and incubated at 45 °C for 3 to 5 h. After incubation, the A_{490} of the samples and standards were then measured using a Genesys 20 spectrophotometer (Thermo Spectronic). A calibration curve was constructed using the readings from the standards and fit to a straight line using Excel. The DDM concentrations of the unknown samples were determined by comparing to the standard curve. The DDM concentrations in the MepA samples were between 0.6% and 1.2% DDM.

2.3. Whole cell activity assays

Cell based assays were performed using JW0451-2 cells (Δ*acrB*, Km^R) provided by the Keio Collection at Yale University. An empty pBAD plasmid along with pBAD plasmids encoding wild-type and D183A MepA were transformed into JW0451-2 cells (Δ*acrB*, Km^R) and grown overnight at 37 °C in LB media supplemented with ampicillin (100 μg/ml) and kanamycin (50 μg/ml). These cultures were used to inoculate 50 ml of LB (1:100 dilution) with ampicillin (100 μg/ml) and kanamycin (50 μg/ml) and grown to an OD_{600} of 0.4. The temperature was then lowered to 28 °C and 0.02% (w/v) of L-arabinose was added to induce expression. After 3 h of induction, cells were collected by centrifugation and washed three times with cell assay buffer (50 mM Tris-HCl, pH 8.0, 150 mM NaCl) at room temperature and resuspended in the same buffer to a final OD_{600} of 1.0. A 1.5 ml aliquot of cell suspension was centrifuged; the supernatant was discarded and the pellet was stored at −20 °C. This sample was used as the zero time point for the assay. Next, 100 μM ethidium bromide was added to the cells at room temperature with stirring and protected from light. Aliquots of 1.5 ml were collected and processed as before at time points of 5, 15, 30, 60 and 90 min. The collected cell pellets were stored at −20 °C. The pellets were thawed and resuspended in 150 μl of assay buffer with 5% (v/v) trichloroacetic acid and vortexed for 30 s. The samples were then centrifuged with a relative centrifugal force (rcf) of 21,100 g at room temperature for 10 min to remove cell debris. Then the supernatants were collected and transferred to a 96-well Microfluor 1 fluorescence plate (Fisher Scientific). The samples were then analyzed in a Spectra Gemini XS fluorescent plate reader (Molecular Devices) with excitation and emission wavelengths set at 484 nm and 630 nm, respectively.

2.4. Fluorescence polarization and intensity binding assay

MepA protein was briefly thawed at room temperature and placed on ice, then concentrated by centrifugation using a 50 k MWCO Amicon Ultracel® (Milipore) at 4 °C to a concentration of ~140 μM. Concentrated protein was then centrifuged at 65 k rpm in a TLA-120.1 rotor at 4 °C for 45 min using an Optima TLX ultracentrifuge (Beckman Coulter) to remove any precipitated protein and to ensure the removal of any aggregation or mis-folded protein. The protein concentration of the supernatant was measured using A_{280}. Calibration using the Amido black assay was performed according to Kaplan and Pedersen [28] to obtain the protein concentration. The amido black assay has been shown to be compatible with lipids and detergents [28–30]. A 40 μl aliquot of the protein sample was set aside and stored at −80 °C for a DDM concentration assay. The binding assays were conducted using approximately 500 μl of buffer B to which 1 μM ethidium bromide was added. Buffer B plus 1 μM ethidium bromide is called “Et buffer”; buffer B plus 1 μM of R6G is called “R6G buffer”; buffer B plus 1 μM of Acr is called “Acr buffer”. Eleven aliquots of 20 μl of Et buffer were dispensed into Eppendorf tubes. Next, 1 μM of ethidium bromide was added to 40 μl of protein sample and then 20 μl of this was mixed into the first 20 μl aliquot of Et buffer. After adequate mixing by pipette, 20 μl was removed and mixed into the next tube containing Et buffer and this process was repeated to perform 2-fold serial dilutions of the protein for all the samples except the final tube which was kept without any protein and contained only Et buffer. The samples were protected from light with aluminum foil and allowed to equilibrate for 20 min at room temperature. The same was done for R6G and Acr binding assays, except using R6G buffer and Acr buffer, respectively.

The samples were analyzed in a FluoroMax-3 (Horiba Jobin) spectrophotometer using a 30 μl QS fluorescence cuvette (1.50 mm, Helma). Changes in the intensity and polarization of ethidium fluorescence were measured using excitation and emission wavelengths of 483 nm and 630 nm, respectively. The excitation and emission bandpasses were both set to 10 nm and integration time was 0.1 s. Fluorescence data for R6G and Acr were measured using excitation wavelengths of 510 nm and 408 nm and emission wavelengths of 555 nm and 450 nm, respectively. The excitation and emission bandpasses were both set to 5 nm for R6G and Acr experiments.

The total fluorescence intensity (F_{Total}) was calculated by combining the polarization components from the polarization experiments as shown in Eq. (1):

$$F_{Total} = VV + 2 \times VH \times G \quad (1)$$

where *VV* and *VH* are the sample's fluorescence polarization components parallel and perpendicular to the excitation light, respectively, and *G* is the G-factor for the instrument specific to the experimental settings of each experiment.

The fluorescence intensity and polarization data were both fitted to a single site binding model:

$$F\ (\text{or FP}) = F_0 + (F_{MAX} - F_0)\ \text{x}\ [Protein]\ /K_D + [Protein] \quad (2)$$

where F (or FP) is the experimentally measured fluorescence intensity (or polarization), F_0 is the fitted fluorescence intensity (or polarization) in the absence of protein, F_{MAX} is the fitted fluorescence intensity (or polarization) when ethidium is fully bound, [*Protein*] is the protein concentration measured in μM, and K_D is the fitted dissociation constant in μM units. Data were processed using the program OriginPro 7.5 using the recorded errors (sd) for weighting the data. For the K_D value determination in the presence of different DDM concentrations, the binding data were collected at concentrations of 0.02, 0.10, 0.30, 0.50, 0.80 and 1.10% DDM by preparing Et, R6G and Acr buffers with the corresponding amount of DDM. The reported errors are the standard deviation of the mean calculated from at least three experiments. The error bars in Figs. 1, 2, and 4–6 are the standard deviations and those in Fig. 3 are the standard deviation of the means. The binding assays in C12E8 were performed as described for DDM, except that Anapoe-C12E8 was used in place of DDM. These binding assays were carried out for two substrates (Acr and R6G) at two concentrations (0.02% and 0.5%) of Anapoe-C12E8.

2.5. DDM binding assays

The effects of DDM on the fluorescence intensity and polarization of Et, R6G and Acr in the absence of protein were determined as follows. Substrate (2 μM for Et and 1 μM for R6G and Acr) was added to 300 μl of assay buffer (50 mM Tris-HCl, pH 8.0, 150 mM NaCl, 2 mM BME) and dispensed into 11 Eppendorf tubes in 20 μl aliquots. Next a 40 μl sample of substrate in assay buffer containing 10% (w/v) DDM was prepared and 20 μl dispensed into a tube and the remaining 20 μl was serially diluted into the tubes containing only assay buffer and substrate. The final tube was left unmixed and contained no detergent. Samples were equilibrated and the fluorescence data collected and analyzed as described in Section 2.4, except that the K_D values resulting from Eq. (2) were expressed in units of % of DDM (w/v) and the term [*Protein*] was replaced with [*DDM*], which is the concentration of DDM in the sample expressed in % (w/v). The reported K_D values are the average of three experiments for Acr and R6G, and of five experiments for Et.

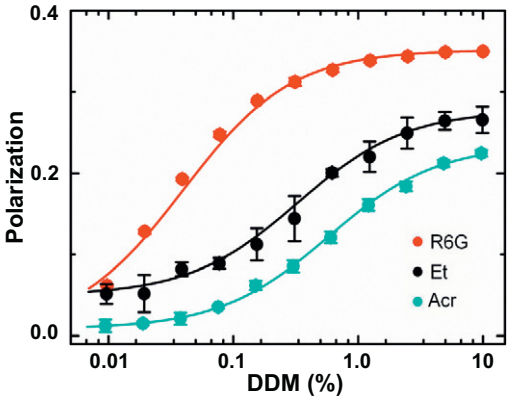

Fig. 1. Substrates binding to DDM micelles as monitored by FP. Representative FP data are shown for the three substrates titrated with DDM. All three substrates show increases in FP with R6G (red) reaching the highest FP value of 0.339 ± 0.005, followed by Et (black) and Acr (cyan) with maximum FP values of 0.269 ± 0.009 and 0.228 ± 0.002, respectively. The detergent concentration is shown on a logarithmic scale.

2.6. Correction of polarization values

The total fluorescence intensity (*F*) of each fluor (1 μM) was measured in the absence and presence of excess MepA protein (approx. 140 μM) using the parallel (*VV*) and perpendicular (*VH*) components from the polarization experiments (Eq. (1)). The total fluorescence intensity, F, of each substrate was measured in three conditions: assay buffer containing 0.02% DDM, assay buffer containing 10% DDM and in the presence of concentrated MepA. From these intensities, the fluorescence enhancement factor, g, was computed as shown in (Eq. (3)) [31–33]:

$$g = F_{(final)}/F_{(initial)} \quad (3)$$

where $F_{(final)}$ represents fluorescence intensity of the bound substrate, and $F_{(initial)}$ is the intensity of the free substrate, according to the output from OriginPro after the data are fitted. We found that only Et showed significant enhancement of fluorescence in the presence of either DDM or MepA and proceeded to correct only the polarization data for Et using Eq. (4) [31–33]:

$$x = (3 - P_b)\left(P_i - P_f\right)/(3 - P_i)\left(P_b - P_f\right) + (g - 1)\left(3 - P_f\right)(P_b - P_i) \quad (4)$$

where *x* represents the fraction of ligand bound, P_f and P_b are the fitted polarization values of free and bound ligand, respectively, P_i is the experimentally observed polarization value and *g* is the fluorescence enhancement factor (Eq. (3)). The corrected values were then fitted to a single site binding model as in Eq. (2).

2.7. Inhibition of Acr, Et & R6G Binding to MepA by TPP

Purified wild-type MepA preparations were ultra-centrifuged as described above for previous polarization binding assays. The inhibition experiments were carried out in buffer B at a MepA concentration of 5 μM, substrate concentration at 1 μM, and decreasing TPP concentration from 7.5 mM to 50 nM, including zero TPP (i.e. no inhibition) sample. Experiments for all three substrates were carried out in triplicate, and the results were averaged and plotted. Excitation and emission wavelengths, as well as band passes, were recorded as described in previous polarization binding assays. Polarization data were fitted to a single site binding model using OriginPro 7.5.

3. Results

3.1. MepA activity assay

To ensure that the wild-type protein is active, we measured the effect of protein expression on the accumulation of Et in *E. coli*. Cells expressing active MepA are expected to accumulate less Et as a result of the efflux activity of MepA. We compared the accumulation of Et in the JW0451-2 cells (Δ*acrB*, Km^R) expressing wild type MepA, D183A, and a control set of JW0451-2 cells (Δ*acrB*, Km^R) transformed with an empty pBAD vector. We found lower accumulation of Et in cells expressing WT MepA than in cells with the D183A mutation in MepA or the pBAD vector alone (Fig. S2). These results are consistent with activity assays done on other MATE transporters [16,17,34,35]. Protein expression and purification of D183A yield a similar amount of protein to that of WT MepA purification (Fig. S2). Cells expressing the D183A construct had a similar amount of Et accumulated as the cells with the control pBAD vector. The D183A mutation has been reported to be inactive in *S. aureus* [23], and our results show that D183A is also inactive in our *E. coli* whole cell assays (Fig. S2).

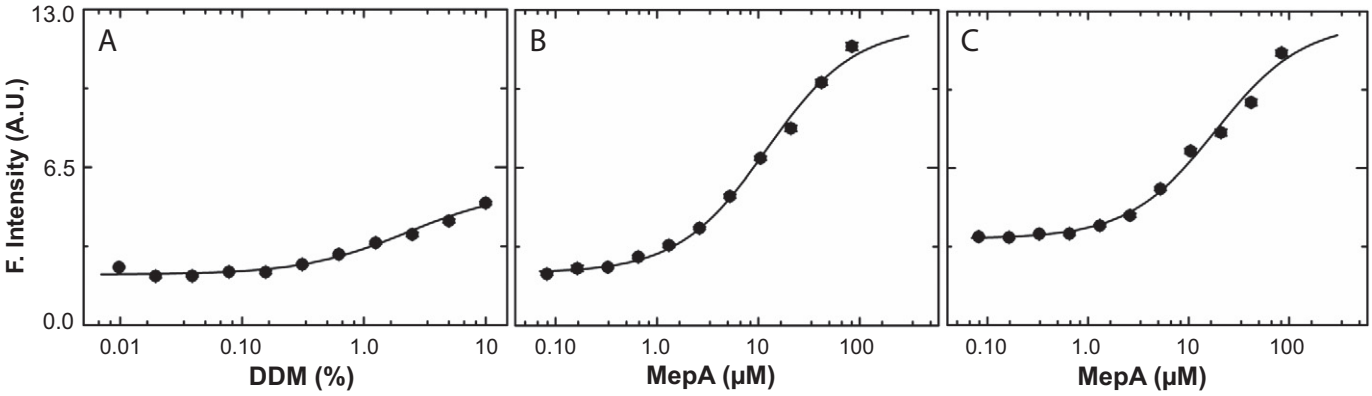

Fig. 2. Enhancement of fluorescence intensity of Et upon binding detergent or MepA. Representative curves of the increase in fluorescence intensity of Et upon binding (**A**) to DDM in the absence of protein, (**B**) to MepA in assay buffer containing 0.02% DDM, and (**C**) to MepA in assay buffer containing 1.1% DDM). The protein and the detergent concentrations are shown on logarithmic scales.

3.2. Interaction between substrates and detergent micelles

Fluorescence polarization (FP) experiments showed that all three substrates interact directly with DDM micelles. The polarization increases from 0.017 to 0.229 for Acr, from 0.032 to 0.339 for R6G, and from 0.062 to a final value of 0.265 for Et (Fig. 1 and Table 1). Similarly, we find that both Acr and R6G interact with C12E8 micelles (Fig. S3). In the case of Et, its interaction with DDM micelles led to enhanced fluorescence intensity, indicating a higher quantum yield for Et upon binding to the detergent. The average observed fluorescence intensity increase for Et was 3.69 ± 0.43 fold (Fig. 2). The average calculated fluorescence intensity increase for Et according to the output from OriginPro after the data were fitted was 3.2 ± 0.2 fold. As a result, the recorded polarization values were corrected as described in the method section (Eq. (4)). This was necessary due to the discrepancy in the quantum yields of the free Et versus the micelle bound Et [31–33].

The association with the DDM micelles can be described as a partitioning of the substrate between the aqueous buffer and the detergent. The partition coefficient (K_{DDM} = [Substrate$_{DDM}$]/[Substrate$_{free}$]) equals 1.0 at the mid-point of the binding curve where half the substrate is bound to micelles and the other half is free in solution. The partition coefficients (K_{DDM}) equaled 1.0 at 0.618% DDM for Acr, 0.036% DDM for R6G, and 0.386% DDM for Et before applying the correction and 1.23% DDM after the correction. Based on the fluorescence enhancement data for Et, we obtained a partition coefficient value of 1.0 at 1.70% DDM. The partition coefficients for C12E8 (K_{C12E8}) equaled 1.0 at 0.218% C12E8 for Acr, and 0.054% C12E8 for R6G (Fig. S3).

3.3. Binding of substrates to MepA and the detergent effect

We find that all three substrates bind to MepA. We carried out the binding experiments between MepA and each of the three substrates at 6 detergent concentrations (0.02, 0.10, 0.30, 0.50, 0.80, and 1.10% DDM), to evaluate the potential interference of the detergent with the binding assays (Fig. 3). We find that the apparent K_D values (K_D^{app}) for all three substrates were influenced by the amount of the detergent used in the assay buffer. Surprisingly, the magnitude of this detergent effect varied greatly among substrates (Figs. 3 and 4, Table 2). We found the detergent effect to be large for R6G, whereas only relatively minor effects were observed for Acr and Et. As a result, the ranking of which substrate binds more tightly to MepA changes with increasing detergent concentration. In order to minimize the detergent effect, typically these binding assays are done in buffers containing low detergent concentrations, such as ~0.02% in the case of DDM. Under this "standard condition", we find that R6G binds to MepA more tightly than Et or Acr. However, at high detergent concentrations (>0.50% DDM) R6G binds to MepA more weakly than Et or Acr. The K_D^{app} increased from the lowest detergent concentration (0.02% DDM) to the highest detergent

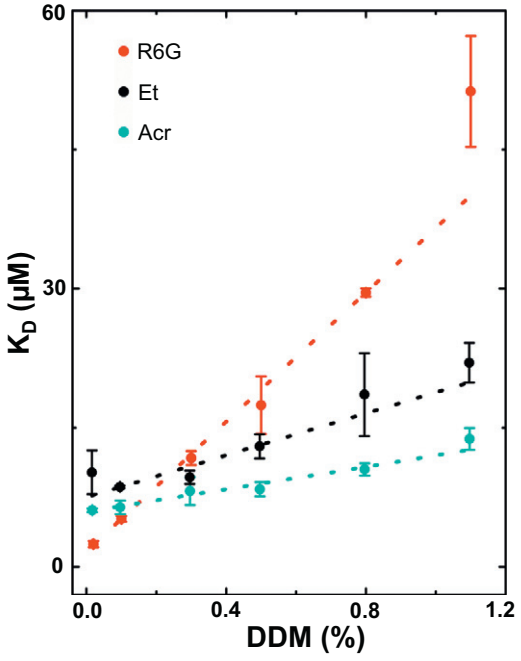

Fig. 3. The detergent effect on measured K_D^{app} values. The affinities of MepA for R6G (red), Et (black) and Acr (cyan) at various DDM concentrations. Significantly, at low DDM concentration (0.02%), MepA appears to interact most tightly with R6G, followed by Acr and Et. Whereas at DDM concentrations ≥0.30%, the relative affinities are reversed with Acr and Et showing stronger interactions than R6G. The apparent K_D of MepA for R6G increases 20.9-fold. The apparent K_D^{app} values for Et and Acr show smaller increases of 2.2 and 2.3 fold, respectively. For Et, the K_D^{app} calculated from the corrected FP data is shown.

Table 1
Interactions between substrates and DDM micelles.

	Acr	R6G	Et
Initial FP	0.017 ± 0.004	0.032 ± 0.002	0.062 ± 0.005
Final FP	0.229 ± 0.017	0.339 ± 0.005	0.265 ± 0.009
DDM (%)[a]	0.618 ± 0.026	0.036 ± 0.005	0.386 ± 0.077[b]
			1.23 ± 0.25[c]
			1.70 ± 0.36[d]

[a] Detergent concentration at K_{DDM} = 1.0.
[b] Calculated from raw polarization data.
[c] Calculated from corrected polarization data.
[d] Calculated from fluorescence enhancement data.

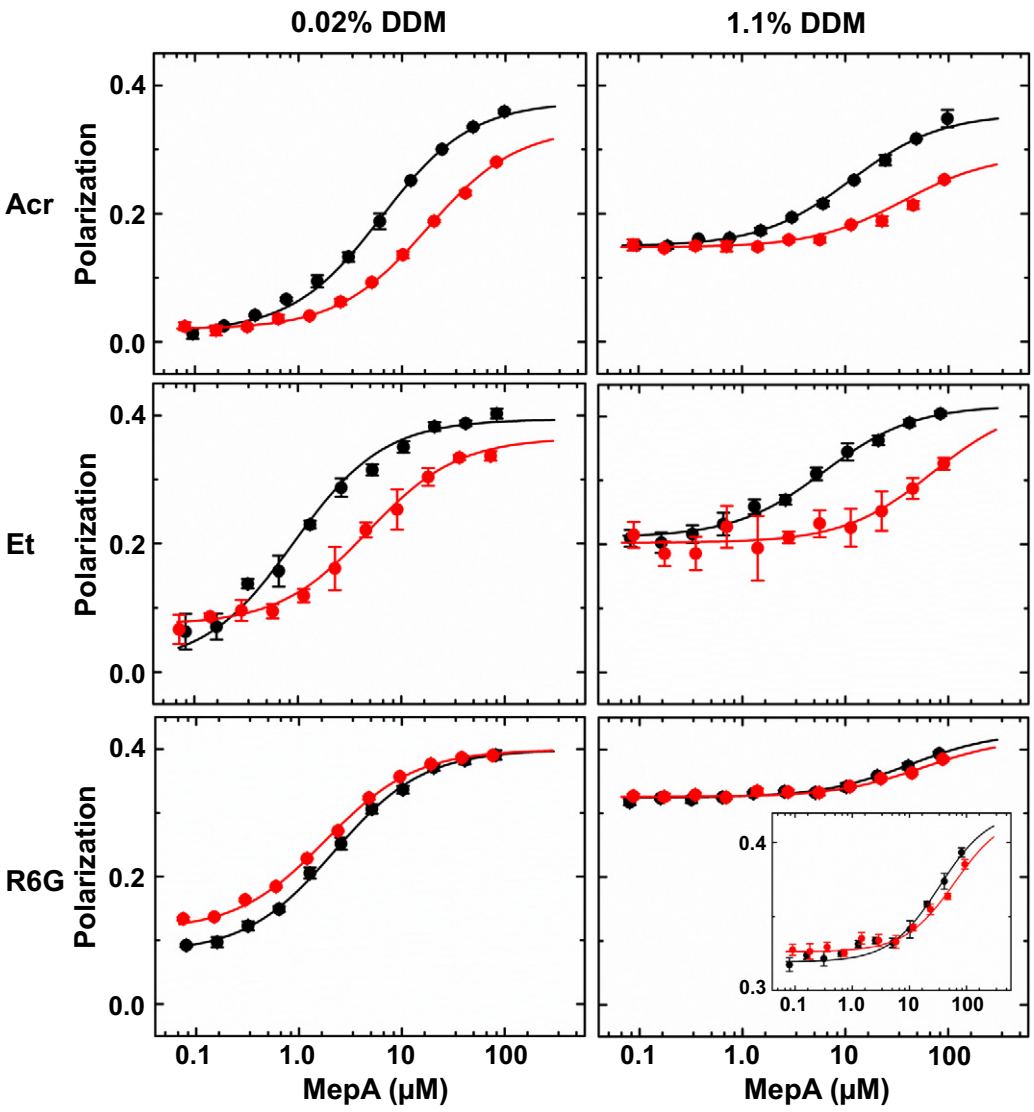

Fig. 4. Substrates binding to WT MepA and D183A at 0.02% and 1.1% DDM. Representative FP data of substrates when titrated with MepA at the lowest and highest DDM concentrations used (0.02% on left; 1.10% on right). Wild type MepA is shown in black and D183A is shown in red. The top panels show data for Acr. The center panels show data for Et, and the bottom panels show data for R6G. The ΔFP for R6G at 1.1% DDM is small, and an inset is included to show the binding curve. The protein concentration is shown on a logarithmic scale.

concentration (1.1% DDM) by 20.9-fold for R6G, 2.3-fold for Acr and 3.3-fold for Et before correction and 2.2-fold after correction (Table 2). A similar increase in the K_D^{app} of 1.8-fold was observed for Et by calculating the K_D^{app} values directly from the fluorescence enhancement data (Fig. S4).

Table 2
Summary of substrates binding affinities to WT MepA and D183A.

Variant	DDM (%)	K_D^{app} (μM)				
		Acr[a]	R6G[a]	Et[a]	Et[b]	Et[c]
WT	0.02	6.0 ± 0.2	2.5 ± 0.1	1.8 ± 0.5	11.2 ± 1.8	10.1 ± 2.3
WT	0.10	6.4 ± 0.7	5.2 ± 0.3	1.9 ± 0.1	8.4 ± 0.4	8.5 ± 0.1
WT	0.30	8.1 ± 1.6	11.8 ± 0.9	2.3 ± 0.3	9.7 ± 0.5	9.6 ± 0.7
WT	0.50	8.3 ± 0.8	17.4 ± 1.1	3.0 ± 0.3	15.0 ± 2.4	12.9 ± 1.3
WT	0.80	10.5 ± 0.6	29.6 ± 3.3	4.4 ± 1.0	15.7 ± 3.0	18.5 ± 4.5
WT	1.10	13.7 ± 1.2	51.3 ± 6.0	5.8 ± 1.0	20.0 ± 1.9	21.9 ± 2.1
D183A	0.02	18.2 ± 0.8	1.8 ± 0.3	4.9 ± 0.1	55.7 ± 9.1	33.3 ± 3.8

[a] Affinities calculated directly from polarization data.
[b] Affinities calculated from total fluorescence intensity.
[c] Affinities calculated from corrected polarization values.

Ethidium presented a special case because its fluorescence increased substantially (up to ~5.2 fold) when fully bound to MepA (Fig. 2). This increase in fluorescence intensity (g) required the application of a correction to the polarization data (Eq. (4)). The value of the enhancement (g) decreased with increasing detergent concentration in the assay buffer (Fig. S4). The quantum yields for Acr and R6G showed small fluctuations that were uncorrelated with the protein or detergent concentrations.

MepA binding assays performed at high detergent concentrations resulted in higher initial FP values. The initial FP values were measured in the absence of protein. The increase in the initial FP values is indicative of association between the substrates and the DDM micelles. The initial FP values increased from 0.013 to 0.145 for Acr, from 0.072 to 0.326 for R6G, and from 0.041 to 0.195 for Et, just as a result of higher detergent concentration in the assay buffer (Fig. 4 and Table 3). Despite higher initial FP values, the addition of MepA resulted in further increases in FP values, reflecting the substrates binding to a larger molecular weight species. The MepA detergent complex is expected to be larger than the free DDM micelles. The final FP values remained approximately the same for all detergent concentrations tested (Fig. 4 and Table 3).

Table 3
Detergent effect on initial and final polarization values.

DDM (%)	Initial FP			Final FP		
	Acr	R6G	Et	Acr	R6G	Et
0.02	0.013 ± 0.002	0.072 ± 0.001	0.041 ± 0.018	0.358 ± 0.001	0.387 ± 0.002	0.385 ± 0.014
0.10	0.040 ± 0.001	0.255 ± 0.007	0.099 ± 0.007	0.360 ± 0.003	0.388 ± 0.002	0.381 ± 0.011
0.30	0.079 ± 0.003	0.298 ± 0.002	0.134 ± 0.001	0.357 ± 0.006	0.393 ± 0.003	0.378 ± 0.012
0.50	0.115 ± 0.006	0.310 ± 0.004	0.160 ± 0.007	0.355 ± 0.006	0.396 ± 0.003	0.379 ± 0.013
0.80	0.122 ± 0.006	0.317 ± 0.001	0.173 ± 0.008	0.351 ± 0.002	0.392 ± 0.002	0.381 ± 0.015
1.10	0.145 ± 0.007	0.326 ± 0.001	0.195 ± 0.012	0.349 ± 0.002	0.394 ± 0.002	0.385 ± 0.012

Binding assays were also carried out in C12E8, in order to determine if the observed detergent effect is specific to DDM, or a more general phenomenon. These experiments were performed on Acr and R6G at two C12E8 concentrations (0.02% and 0.5%). We observed that at higher C12E8 concentration, the K_D^{app} increased for both substrates (Acr and R6G). Interestingly, again we found that R6G was more greatly influenced by the change in the detergent concentration than Acr (Fig. 5). The K_D^{app} increased by 8.0-fold for R6G binding and by 3.5-fold for Acr binding over a concentration range of 0.02% to 0.5% C12E8. In many of the experiments carried out at higher detergent concentrations saturations were not reached due to the lowered affinity. As a result the precision of reported K_D^{app} values is less reliable in the cases of low binding affinities.

3.4. D183A binding

The D183A mutation has been shown previously to be inactive in *S. aureus* [23]. To investigate whether D183A affects binding, and whether the FP binding assay used here is sensitive enough to detect the potential effects of mutations on binding, we measured binding affinities of all three substrates to the D183A mutant MepA protein. Compared to the wild type protein, we find that D183A has weaker binding with both Acr and Et (Fig. 4 and Table 2). To probe for potential detergent interference, we measured the binding to D183 both at the lowest DDM concentration (0.02%) and at the highest (1.10%). Binding of D183A MepA to Acr and Et was weaker than wild type MepA at both detergent concentrations (Fig. 4). In the case of R6G, no effect on binding was observed as a result of the D183A mutation.

3.5. Inhibition assay

To confirm that we are observing substrate binding to a specific MepA site, we carried out an inhibition experiment with TPP. We observe a loss of FP with increasing concentrations of TPP for all three substrates (Fig. 6). This is consistent with results observed for TPP inhibition of R6G binding to NorM [36]. The inhibition data reflect that TPP competes out all three substrates from a specific binding site.

4. Discussion

Here we report the first expression, purification and characterization of the *S. aureus* multidrug transporter MepA. We examined the effect of detergent on the binding between MepA and three of its substrates, and we found that the effect of the detergent concentration was highly substrate dependent. The detergent concentration had a large impact on the binding of R6G to MepA, and only a slight effect on the binding of Acr and Et to MepA. All three substrates showed an upward trend in the K_D^{app} values with increasing detergent concentration. The increases in the K_D^{app} values fit a linear relationship with the concentration of the detergent (Fig. 3). The slopes of these lines reflect the extent of the "detergent effect" on binding. Acr and Et have similar slopes with modest inclines, whereas a significantly larger incline was observed for R6G.

Increasing the detergent concentration can impact the behavior of both the protein as well as the substrate. However, the effect on K_D^{app} values appears to be mainly a result of the influence of the detergent on the substrates, since the effect is highly substrate dependent.

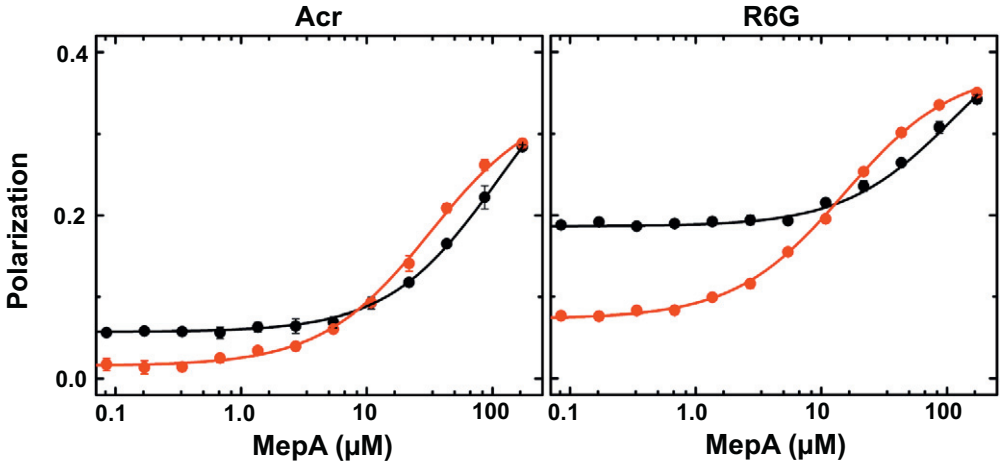

Fig. 5. The detergent effect on measured K_D^{app} values in C12E8. The K_D^{app} values between Acr and MepA (left panel) increased 3.5-fold from 31.3 ± 3.6 to 109.1 ± 3.5 μM when the C12E8 concentration is increased from 0.02% (red) to 0.5% (black). The K_D^{app} values between R6G and MepA (right panel) increased 8.0 fold from 14.0 ± 0.7 to 111.8 ± 17.6 μM when the C12E8 concentration is increased from 0.02% (red) to 0.5% (black).

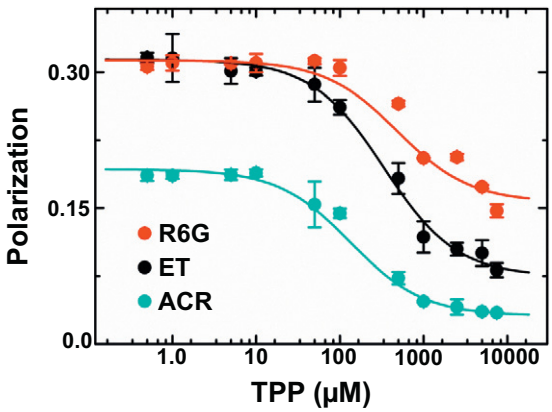

Fig. 6. Inhibition assay. Inhibition of Acr (cyan), Et (black), and R6G (red) binding to WT MepA using TPP. The TPP concentration is shown on a logarithmic scale.

Additionally, the magnitudes of the slopes correlate with the affinities of the substrates to the detergent micelles themselves (Fig. 1). Comparing the assays done at 1.1% DDM to those done at 0.02% DDM it was revealed that the K_D^{app} values for Acr, Et, and R6G change by 2.3, 2.2 and 20.9 fold, respectively. As a result of the considerably differing extents of detergent effect, an important observation comes into light. At lower detergent concentrations, R6G appears to have a higher affinity for MepA than either Acr or Et. However, at higher DDM concentrations, Acr and Et have a higher affinity for MepA than R6G. The implications of this reversal in relative affinities can be significant for drug design. A similar behavior is observed in another detergent (C12E8), with R6G having a bigger change in K_D^{app} than that measured for Acr upon binding to MepA as a result of increasing the detergent concentration. Additionally, differences in the K_D^{app} were observed depending on the detergent used (DDM vs. C12E8). This highlights that the K_D^{app} can be dependent on the detergent selected for the experiments in addition to the concentration of the detergent.

Previously reported affinities between multidrug transporters and their substrates are in the range observed for MepA at low detergent concentration (0.02% DDM) [18,36–38]. Additionally, the ranking of substrates is also the same as what we observe at lowest detergent concentration (0.02% DDM), with R6G appearing to have the highest affinity toward the various transporters. For example, AcrB was shown to have K_D values of 5.5 ± 0.9 μM and 8.7 ± 1.9 μM toward R6G and Et, respectively [37]. The MATE transporters NorM and YdhE also behaved similarly. NorM was reported to have K_Ds of 3.4 ± 0.2 μM and 12.3 ± 1.3 μM to R6G and Et, respectively, and YDhE was reported to have K_Ds of 3.0 ± 0.2 μM and 9.8 ± 0.9 μM to R6G and Et, respectively [36].

Prior assessments of detergent influence on substrate binding in similar systems have had varying results. It was reported that the detergent had no effect on NorM or YdhE's binding to R6G [36], and little effect on AcrB binding to R6G [37]. A different aspect of the impact of the detergent was observed for EmrE. Changing the detergent from DDM to nonyl-glucoside had a large effect on the affinity of EmrE (12–26 fold) toward TPP [39]. Other reports suggest that detergents can block substrate binding [40,41]. Based on the literature and results reported here, we find that although the detergent effect may be common, it is not universal. Therefore, it is important to examine each membrane protein with each substrate and detergent combination individually. Results from other membrane protein systems support this conclusion. For example, the detergent concentration was shown to influence protein stability in the case of FsrC [42]. Additionally, in the case of the multidrug transporter SugE, it was shown that interactions with the ligands were detergent-dependent [43].

Ethidium presented a special case, because its fluorescence intensity increased as a result of binding to MepA or to DDM micelles. Due to this increase in quantum yield, the fluorescence of the bound Et was stronger than the fluorescence of the free Et, which skewed the polarization signal. Therefore, we corrected the polarization data removing the bias introduced by the enhanced fluorescence intensities [31–33]. As a result, not only does an increase in DDM concentration influence the apparent K_D^{app}, but it also affects the correction factor applied to the FP data (Fig. S4).

The increase of the quantum yield of Et is not unusual. It has been previously reported that water molecules quench the fluorescence of Et, so when Et is in a hydrophobic environment its measured fluorescence intensity increases [44]. Therefore, this quantum yield enhancement is not limited to MepA binding but is expected to be a general fluorescence property of Et. The K_D^{app} values changed substantially upon applying the correction factor. For example, at 0.02% DDM the K_D^{app} was corrected from 2.7 μM to 15.5 μM. Consequently, it is essential to consider changes in the quantum yield when taking polarization measurements. At the same time, the increase in fluorescence offered additional data to observe the binding process. The increase in fluorescence appeared to be a direct consequence of binding to MepA and here it was demonstrated that it can be effectively used for the measurement of apparent K_D values. Remarkably, the Et K_D^{app} values that were measured from the enhancement data were in large agreement with those obtained from the corrected FP experiments (Fig. S4). Therefore, the change in the fluorescence intensity of Et requires the correction of FP data, and at the same time it can also offer an additional tool for monitoring the binding event.

The MepA D183A mutation showed a similar degree of lowered affinity toward Acr and Et, but no apparent effect on R6G binding (Table 2). A number of recent structures of MATE proteins have been determined, some with their substrates bound [18–20]. In all these structures the corresponding position for D183A is not close to the substrate binding site [23]. It is plausible that in a new uncharacterized protein conformation, D183A may interact directly with the substrates. However, the available structural data suggest that D183A does not interact with the substrates, and therefore the influence of D183A on substrate binding may be due to conformational effects or indirect interactions. Although FP is commonly used to measure the binding of hydrophobic substrates to various MATE transporters, the detection of the effect of mutations on binding using FP is novel to these systems. Here we show that FP is sensitive enough to detect the effects of a point mutation on substrate binding, however this sensitivity may be substrate dependent. The lack of effect on R6G binding may be due to the high detergent effect which may mask the effect of the mutation. We find that binding assays done with Acr and Et may be more sensitive to the effects of mutations on binding. This is the first report using FP to observe the effect of a mutation on substrate binding for any MATE transporter.

5. Conclusions

We determined the affinity of MepA to three of its substrates at various detergent concentrations. We find that the detergent interference is highly substrate specific. In the case of MepA, we demonstrated that Acr and Et were only slightly influenced by the detergent concentration, whereas R6G was highly sensitive. We also showed that the affinity of the substrate to the detergent correlates with the degree of the detergent effect on binding. Similar behavior was observed when C12E8 was used as a detergent. We find that the effect of the detergent on the binding of a hydrophobic substrate to a membrane protein needs to be examined on a case-by-case basis. We showed that D183 is important for substrate binding, despite being distant from the predicted binding site. We also find that the FP assays can be sensitive enough to detect the effects of point mutations on binding.

Acknowledgements

We thank Professors Robert Nakamoto and Owen Pornillos for critical reading of the manuscript.

Appendix A. Supplementary data

Supplementary data to this article can be found online at http://dx.doi.org/10.1016/j.bbamem.2014.06.013.

References

[1] X.Z. Li, H. Nikaido, Efflux-mediated drug resistance in bacteria: an update, Drugs 69 (2009) 1555–1623.
[2] R.D. Cannon, E. Lamping, A.R. Holmes, K. Niimi, P.V. Baret, M.V. Keniya, K. Tanabe, M. Niimi, A. Goffeau, B.C. Monk, Efflux-mediated antifungal drug resistance, Clin. Microbiol. Rev. 22 (2009) 291–321.
[3] Y.J. Chung, M.H. Saier Jr., SMR-type multidrug resistance pumps, Curr. Opin. Drug Discov. Devel. 4 (2001) 237–245.
[4] H. Nikaido, Structure and mechanism of RND-type multidrug efflux pumps, Adv. Enzymol. Relat. Areas Mol. Biol. 77 (2011) 1–60.
[5] M.A. Seeger, H.W. van Veen, Molecular basis of multidrug transport by ABC transporters, Biochim. Biophys. Acta 1794 (2009) 725–737.
[6] O. Lewinson, J. Adler, N. Sigal, E. Bibi, Promiscuity in multidrug recognition and transport: the bacterial MFS Mdr transporters, Mol. Microbiol. 61 (2006) 277–284.
[7] H. Omote, M. Hiasa, T. Matsumoto, M. Otsuka, Y. Moriyama, The MATE proteins as fundamental transporters of metabolic and xenobiotic organic cations, Trends Pharmacol. Sci. 27 (2006) 587–593.
[8] Y. Morita, K. Kodama, S. Shiota, T. Mine, A. Kataoka, T. Mizushima, T. Tsuchiya, NorM, a putative multidrug efflux protein, of *Vibrio parahaemolyticus* and its homolog in *Escherichia coli*, Antimicrob. Agents Chemother. 42 (1998) 1778–1782.
[9] Y. Morita, A. Kataoka, S. Shiota, T. Mizushima, T. Tsuchiya, NorM of *Vibrio parahaemolyticus* is an Na(+)-driven multidrug efflux pump, J. Bacteriol. 182 (2000) 6694–6697.
[10] M.N. Huda, Y. Morita, T. Kuroda, T. Mizushima, T. Tsuchiya, Na + -driven multidrug efflux pump VcmA from *Vibrio cholerae* non-O1, a non-halophilic bacterium, FEMS Microbiol. Lett. 203 (2001) 235–239.
[11] J. Chen, Y. Morita, M.N. Huda, T. Kuroda, T. Mizushima, T. Tsuchiya, VmrA, a member of a novel class of Na(+)-coupled multidrug efflux pumps from *Vibrio parahaemolyticus*, J. Bacteriol. 184 (2002) 572–576.
[12] M.N. Huda, J. Chen, Y. Morita, T. Kuroda, T. Mizushima, T. Tsuchiya, Gene cloning and characterization of VcrM, a Na + -coupled multidrug efflux pump, from *Vibrio cholerae* non-O1, Microbiol. Immunol. 47 (2003) 419–427.
[13] X.J. Xu, X.Z. Su, Y. Morita, T. Kuroda, T. Mizushima, T. Tsuchiya, Molecular cloning and characterization of the HmrM multidrug efflux pump from *Haemophilus influenzae* Rd, Microbiol. Immunol. 47 (2003) 937–943.
[14] L. Dridi, J. Tankovic, J.C. Petit, CdeA of *Clostridium difficile*, a new multidrug efflux transporter of the MATE family, Microb. Drug Resist. 10 (2004) 191–196.
[15] A. Begum, M.M. Rahman, W. Ogawa, T. Mizushima, T. Kuroda, T. Tsuchiya, Gene cloning and characterization of four MATE family multidrug efflux pumps from *Vibrio cholerae* non-O1, Microbiol. Immunol. 49 (2005) 949–957.
[16] X.Z. Su, J. Chen, T. Mizushima, T. Kuroda, T. Tsuchiya, AbeM, an H + -coupled *Acinetobacter baumannii* multidrug efflux pump belonging to the MATE family of transporters, Antimicrob. Agents Chemother. 49 (2005) 4362–4364.
[17] G.X. He, T. Kuroda, T. Mima, Y. Morita, T. Mizushima, T. Tsuchiya, An H(+)-coupled multidrug efflux pump, PmpM, a member of the MATE family of transporters, from *Pseudomonas aeruginosa*, J. Bacteriol. 186 (2004) 262–265.
[18] X. He, P. Szewczyk, A. Karyakin, M. Evin, W.X. Hong, Q. Zhang, G. Chang, Structure of a cation-bound multidrug and toxic compound extrusion transporter, Nature 467 (2010) 991–994.
[19] M. Lu, J. Symersky, M. Radchenko, A. Koide, Y. Guo, R. Nie, S. Koide, Structures of a Na + -coupled, substrate-bound MATE multidrug transporter, Proc. Natl. Acad. Sci. U. S. A. 110 (2013) 2099–2104.
[20] Y. Tanaka, C.J. Hipolito, A.D. Maturana, K. Ito, T. Kuroda, T. Higuchi, T. Katoh, H.E. Kato, M. Hattori, K. Kumazaki, T. Tsukazaki, R. Ishitani, H. Suga, O. Nureki, Structural basis for the drug extrusion mechanism by a MATE multidrug transporter, Nature 496 (2013) 247–251.
[21] A.A. Huet, J.L. Raygada, K. Mendiratta, S.M. Seo, G.W. Kaatz, Multidrug efflux pump overexpression in *Staphylococcus aureus* after single and multiple in vitro exposures to biocides and dyes, Microbiology 154 (2008) 3144–3153.
[22] G.W. Kaatz, F. McAleese, S.M. Seo, Multidrug resistance in *Staphylococcus aureus* due to overexpression of a novel multidrug and toxin extrusion (MATE) transport protein, Antimicrob. Agents Chemother. 49 (2005) 1857–1864.
[23] B.D. Schindler, D. Patel, S.M. Seo, G.W. Kaatz, Mutagenesis and modeling to predict structural and functional characteristics of the *Staphylococcus aureus* MepA multidrug efflux pump, J. Bacteriol. 195 (2013) 523–533.
[24] Y. Sonoda, S. Newstead, N.J. Hu, Y. Alguel, E. Nji, K. Beis, S. Yashiro, C. Lee, J. Leung, A.D. Cameron, B. Byrne, S. Iwata, D. Drew, Benchmarking membrane protein detergent stability for improving throughput of high-resolution X-ray structures, Structure 19 (2010) 17–25.
[25] S. Newstead, S. Ferrandon, S. Iwata, Rationalizing alpha-helical membrane protein crystallization, Protein Sci. 17 (2008) 466–472.
[26] pBAD/His A, B, and C pBAD/Myc-His A, B, and C, http://tools.lifetechnologies.com/content/sfs/manuals/pbad_man.pdf , can also be found at http://people.virginia.edu/~sf3bb/pbad_man.pdf , Invitrogen.
[27] A. Urbani, T. Warne, A colorimetric determination for glycosidic and bile salt-based detergents: applications in membrane protein research, Anal. Biochem. 336 (2005) 117–124.
[28] R.S. Kaplan, P.L. Pedersen, Determination of microgram quantities of protein in the presence of milligram levels of lipid with amido black 10B, Anal. Biochem. 150 (1985) 97–104.
[29] W. Schaffner, C. Weissmann, A rapid, sensitive, and specific method for the determination of protein in dilute solution, Anal. Biochem. 56 (1973) 502–514.
[30] R.A. Figler, H. Omote, R.K. Nakamoto, M.K. Al-Shawi, Use of chemical chaperones in the yeast *Saccharomyces cerevisiae* to enhance heterologous membrane protein expression: high-yield expression and purification of human *P*-glycoprotein, Arch. Biochem. Biophys. 376 (2000) 34–46.
[31] G. Mocz, M.K. Helms, D.M. Jameson, I.R. Gibbons, Probing the nucleotide binding sites of axonemal dynein with the fluorescent nucleotide analogue 2'(3')-*O*-(-*N*-methylanthraniloyl)-adenosine 5'-triphosphate, Biochemistry 37 (1998) 9862–9869.
[32] D.M. Jameson, G. Mocz, Fluorescence polarization/anisotropy approaches to study protein–ligand interactions: effects of errors and uncertainties, Methods Mol. Biol. 305 (2005) 301–322.
[33] D.M. Jameson, J.A. Ross, Fluorescence polarization/anisotropy in diagnostics and imaging, Chem. Rev. 110 (2010) 2685–2708.
[34] M. Otsuka, M. Yasuda, Y. Morita, C. Otsuka, T. Tsuchiya, H. Omote, Y. Moriyama, Identification of essential amino acid residues of the NorM Na+/multidrug antiporter in *Vibrio parahaemolyticus*, J. Bacteriol. 187 (2005) 1552–1558.
[35] K. Hashimoto, W. Ogawa, T. Nishioka, T. Tsuchiya, T. Kuroda, Functionally cloned pdrM from *Streptococcus pneumoniae* encodes a Na(+) coupled multidrug efflux pump, PLoS One 8 (2013) e59525.
[36] F. Long, C. Rouquette-Loughlin, W.M. Shafer, E.W. Yu, Functional cloning and characterization of the multidrug efflux pumps NorM from *Neisseria gonorrhoeae* and YdhE from *Escherichia coli*, Antimicrob. Agents Chemother. 52 (2008) 3052–3060.
[37] C.C. Su, E.W. Yu, Ligand-transporter interaction in the AcrB multidrug efflux pump determined by fluorescence polarization assay, FEBS Lett. 581 (2007) 4972–4976.
[38] K.A. Hassan, Z. Xu, R.E. Watkins, R.G. Brennan, R.A. Skurray, M.H. Brown, Optimized production and analysis of the staphylococcal multidrug efflux protein QacA, Protein Expr. Purif. 64 (2009) 118–124.
[39] Y.J. Chen, O. Pornillos, S. Lieu, C. Ma, A.P. Chen, G. Chang, X-ray structure of EmrE supports dual topology model, Proc. Natl. Acad. Sci. U. S. A. 104 (2007) 18999–19004.
[40] M. Quick, L. Shi, B. Zehnpfennig, H. Weinstein, J.A. Javitch, Experimental conditions can obscure the second high-affinity site in LeuT, Nat. Struct. Mol. Biol. 19 (2012) 207–211.
[41] T. Zordan-Nudo, V. Ling, Z. Liu, E. Georges, Effects of nonionic detergents on *P*-glycoprotein drug binding and reversal of multidrug resistance, Cancer Res. 53 (1993) 5994–6000.
[42] S.G. Patching, S. Edara, P. Ma, J. Nakayama, R. Hussain, G. Siligardi, M.K. Phillips-Jones, Interactions of the intact FsrC membrane histidine kinase with its pheromone ligand GBAP revealed through synchrotron radiation circular dichroism, Biochim. Biophys. Acta 1818 (2012) 1595–1602.
[43] D.C. Bay, R.J. Turner, Spectroscopic analysis of the intrinsic chromophores within small multidrug resistance protein SugE, Biochim. Biophys. Acta 1808 (2011) 2233–2244.
[44] J. Olmsted III, D.R. Kearns, Mechanism of ethidium bromide fluorescence enhancement on binding to nucleic acids, Biochemistry 16 (1977) 3647–3654.